The Effects of Mode Impurity on Ka-Band System Performance

D. J. Hoppe, W. A. Imbriale, and A. M. Bhanji
Radio Frequency and Microwave Subsystems Section

Problems associated with spurious mode generation in the proposed Ka-Band gyroklystron transmitter tube, overmoded transmission line, and feed are discussed. A brief description of the overall problem is presented. The theory used to evaluate feed and antenna performance when spurious modes are present is given. Results for feed patterns and overall antenna patterns for various levels and types of spurious modes are presented. Worst case antenna efficiency is calculated as a function of spurious mode level. Conclusions are drawn regarding the results of this study and their application to specifications on the transmitter tube and transmission line system.

I. Introduction

A conceptual design for a 400 kW CW Ka-Band (34 GHz) transmitter system has been presented in a previous report (Ref. 1). Conventional klystron amplifiers and dominant mode transmission systems are not well suited for high-power millimeter wavelength systems since the small surface areas and high losses in these devices require cooling which is beyond the state of the art at this time. A solution to this problem is provided by using a gyroamplifier and overmoded transmission system (Ref. 2) which is shown in Fig. 1. In the proposed system, the microwave power is extracted from the beam in an overmoded cavity and delivered to the antenna feed in overmoded circular waveguide. Once the microwave power is extracted from the beam it enters a ripple wall mode converter which converts most of the power from the higher order TE_{12} mode into the TE_{11} mode. The microwave power then passes through a tapered collector region in the tube, out the vacuum window, through another taper and the transmission line, and is radiated out the antenna feed. Each of these components allows multimode propagation; for example, the transmission line allows 66 waveguide modes to propagate. Although a well-designed tube and transmission system will minimize mode conversion in these components, the microwave power at the input to the feed will no longer be contained in the dominant TE_{11} waveguide mode. Since all of the microwave systems used previously in the DSN were single mode systems, this problem is particular to the Ka-band system. This report describes a theoretical study which was undertaken to determine the effect of mode purity on antenna performance.

The first section of the report describes the theory used and some of the basic equations involved, as well as the computer codes used to perform the calculations. The results of the calculations are presented, and conclusions are drawn regarding the results of this study and their application to system specifications.

II. Theory

A. Description of the Problem

The feed and Cassegrain system are shown schematically in Fig. 2. The problem we wish to solve is the following: Given a fixed amount of microwave power incident at the input of the overmoded feed at point A, how does the Effective Isotropically Radiated Power (EIRP) of the antenna system vary depending on the mode content of this incident microwave power?

The overall problem is solved by breaking it up into sections. First of all, the feed section is analyzed in a manner which gives, for any incident electric field $\mathbf{E}_A^i$ at point A, the resulting reflected field $\mathbf{E}_A^r$ at A, and the field present in the aperture of the feed $\mathbf{E}_B$. The electric field in the feed is described as a combination of circular waveguide modes. The far field of the feed $\mathbf{E}_C$, which is incident on the subreflector at surface C, is then determined from the feed aperture field $\mathbf{E}_B$. The field incident on the subreflector is then scattered into the field illuminating the paraboloid, $\mathbf{E}_D$, by using the geometrical theory of diffraction (GTD). Finally, the resulting far field $\mathbf{E}_E$ is determined from the fields on the paraboloid by physical optics using a Jacobi-Bessel expansion technique.

The question arises as to which types of spurious modes should be considered. The main part of the microwave power will be carried by a TE_{11} mode which is rotating in the right-hand sense. Symmetric diameter changes, i.e., tapers, couple this mode only to right-hand rotating TE_{1n} and TM_{1n} modes. These are the only types of spurious modes we would expect to be present at the field input if perfect circularity in the system were maintained, as well as perfect alignment and straightness. It is expected that although perfection will not be maintained with respect to these parameters the bulk of the spurious power will be contained in the TE_{1n} and TM_{1n} modes. Therefore, the detailed analysis will be limited only to modes with one azimuthal variation. Assuming the TE_{11} mode carries most of the microwave power, the modes most strongly coupled due to deformations other than symmetric radial deformations may be determined. The right-hand rotating TE_{11} mode is coupled to the TE_{01} mode through curvature, discrete waveguide tilts, and waveguide offsets. Ellipticity in the waveguide causes coupling to the left-hand rotating TE_{11} mode as well as right-hand rotating TE_{3n} and TM_{3n} modes. Approximate results for the effects of these modes on antenna performance will be given at the end of the results section.

B. Feed Analysis

A cut-away view and cross sectional view of the antenna feed are shown in Fig. 3. The inside diameter of the overmoded transmission line was chosen to be 1.75 in. which is approximately the same size as the output of the X-band hybrid horns when scaled to 34 GHz. Therefore the Ka-band system requires no flare angle horn, but merely a straight section of corrugated waveguide with varying slot depth. The slot depth profile is chosen to transform the TE_{11} mode of the smooth-walled waveguide into the balanced HE_{11} mode, which is one of the modes which exists in a corrugated waveguide with constant slot depth. Care must be taken in the design of this transition section since many other modes may also be excited in the 1.75-in. diameter corrugated waveguide at this frequency. The section's length and slot depth profile were adjusted to nearly optimally illuminate the subreflector when a pure TE_{11} mode was incident at point A. Along with the TE_{11} mode 8 other modes with one azimuthal variation may propagate in 1.75-in. diameter waveguide at 34 GHz. They are TE_{1n} (n = 2, 3, 4, 5) and TM_{1n} (n = 1, 2, 3, 4). The feed response to any combination of these modes at the input A is required.

The corrugated section is analyzed using a new computer code developed for the Ka-Band project.[1] The analysis follows the method of James (Ref. 3), expanding the fields inside each fin and slot in terms of circular waveguide modes, and matching the fields at each slot-fin boundary. All of the possible propagating modes, as well as a sufficient number of evanescent modes are matched at each edge, with results for successive edges and waveguide lengths being cascaded as one moves through the device. In this way the interaction between the fields of non-adjacent as well as adjacent slots is taken into account. The result of the calculation is a matrix equation relating the reflected and aperture modes to the input modes. If $\mathbf{a}_1$ is a vector containing the power normalized amplitudes of the input modes, then we may calculate the reflected modes $\mathbf{b}_1$, and the aperture modes $\mathbf{b}_2$ using

$$\mathbf{b}_2 = [S_{21}]\,\mathbf{a}_1 \tag{1}$$

$$\mathbf{b}_1 = [S_{11}]\,\mathbf{a}_1 \tag{2}$$

Here $[S_{21}]$ and $[S_{11}]$ are the scattering matrices resulting from the computer run. They depend only on frequency and device dimensions, not input modes. We may therefore specify any input vector $\mathbf{a}_1$ and calculate the reflected and aperture fields.

Using the normalized amplitudes calculated above, and the normalized vector functions giving the field distributions for each mode, we find the aperture field $\mathbf{E}_B$. The far field is then calculated by the method described by Silver and Ludwig (Ref. 4, 5).

[1] See D. J. Hoppe, "Scattering Matrix Program for Circular Waveguide Junctions," Interoffice Memorandum #3335-84-071 (internal document), Dec. 5, 1984, Jet Propulsion Laboratory, Pasadena, Calif.

$$\mathbf{E}_c = \frac{-1}{4\pi} \iint_S (-j\mu\omega(\mathbf{a}_n \times \mathbf{H}_B)\,\phi + (\mathbf{a}_n \times \mathbf{E}_B) \times \nabla\phi)\,ds \tag{3}$$

where

$\mathbf{E}_B$ = aperture electric field

$\mathbf{H}_B$ = aperture magnetic field

$\mathbf{a}_n$ = unit vector normal to aperture surface

dS = incremented area on aperture surface

$\omega = 2\pi f$

f = frequency

μ = free space permiability

∇ = gradient operator

$\phi = (\exp - jkr)/r$

$k = 2\pi/\lambda o$

r = far field point distance from origin (spherical radius)

When $\mathbf{E}_B$ is represented in terms of circular waveguide modes the resulting integrals have already been evaluated by Silver (Ref. 5). Therefore, given an input vector and the scattering matrix, we determine the aperture modes and composite far field patterns. Throughout the analysis care must be taken to ensure proper normalization of the field amplitudes in terms of power.

C. Dual Reflector Antenna Analysis

Given the feedhorn field $\mathbf{E}_C$ which is incident on the subreflector, the GTD/Jacobi-Bessel Program (Ref. 6) was used to calculate the far field pattern of the composite Cassegrain system.

The field scattered to the parabolic main reflector from the ellipsoidal subreflector is calculated using GTD. The field incident on the paraboloid $\mathbf{E}_D$, is then integrated into the resulting final far field pattern of the antenna. In the final integral's evaluation a Jacobi-Bessel expansion technique is used (Ref. 7). In this study the far field patterns for the present 64-meter system were examined for arbitrary excitation of the feed. It should be pointed out that very accurate modeling of the 64-meter system is possible with the GTD/Jacobi-Bessel program, and effects such as the slight offsets of the feed placement and subreflector are included.

This completes the explanation of the analysis method. The total far field, including the on-axis field $\mathbf{E}_E$, may now be determined for arbitrary feed excitation.

D. Gain and Orthogonality

Since the circular waveguide modes at the input to the feed are power orthogonal, we may calculate the far field for any arbitrary combination of mode amplitudes and phases by knowing the antenna pattern for each of the modes individually. An explanation follows.

Each waveguide mode incident on the feed generates a set of modes in the feed aperture. Since the feed and antenna are assumed to be lossless in the analysis, the set of aperture modes generated by any pure waveguide mode at the input is orthogonal to the set generated by any other pure waveguide mode at the input. This is a property of the scattering matrix determined from the fact that the device is lossless and power must be conserved (Ref. 8). Also antenna gain and directivity are equivalent. Power must also be conserved in the far field of the feed. That is, the far field generated by 1 watt of TE_{11} incident power contains 1 watt (neglecting reflections); the far field of 1 watt of TM_{11} incident also contains 1 watt; and since the two exciting modes are power orthogonal, the far field produced by the sum will contain 2 watts. This was confirmed by numerically integrating far-field patterns for single modes exciting the feed and arbitrary combinations. This result gives confidence in the correctness of the far-field calculations. Two different waveguide modes exciting the feed act like a two-element array with no mutual coupling.

Returning to the notation of part B we excite the feed with a single mode, mode number i ($i = 1, 2, \ldots, 9$). The fields are normalized so that we have for the input power $P(i)$

$$P(i) = |a_1(i)|^2 \tag{4}$$

For this input signal we then calculate the feed pattern, subreflector pattern, and finally the electric field on the antenna axis, $\mathbf{E}_E(i)$. If we separate out the vector nature of the field, letting $\mathbf{a}$ be a unit vector in the direction of the field,

$$\mathbf{E}_E(i) = \frac{\mathbf{E}_E(i)\mathbf{a}}{r\sqrt{4\pi}} \tag{5}$$

We may calculate the gain for the specific input mode, $G(i)$

$$G(i) = \frac{|E_E(i)|^2}{\eta P(i)} = \frac{|E_E(i)|^2}{\eta\,|a_1(i)|^2} \tag{6}$$

or

$$E_E(i) = \eta |a_1(i)| G(i) \exp j\Phi(i) \tag{7}$$

where $\Phi(i)$ is the phase of the far field which is given by the analysis but lost in the gain calculation. The gain for each

input mode may be calculated similarly. When an arbitrary combination excites the feed we have

$$P_{\text{sum}} = \sum_i |a_1(i)|^2 \tag{8}$$

$$E_{\text{sum}} = \sum_i E_E(i) = \sum_i \eta |a_1(i)| G(i) \exp j\Phi(i) \tag{9}$$

The antenna gain for any excitation of the feed is given by

$$G_{\text{sum}} = \frac{|E_{\text{sum}}|^2}{\eta P_{\text{sum}}} \tag{10}$$

or

$$G_{\text{sum}} = \frac{\left| \sum_i a_1(i) |G(i) \exp j\Phi(i)|^2 \right|}{\sum_i |a_1(i)|^2}$$

The next section will describe the results of the calculations described above.

III. Results

A. Feed Patterns

The calculations described in Sec. II part B were carried out for a preliminary feed design. The feed radiation pattern for each possible input mode was determined. A few examples of the results of these calculations are depicted in Figs. 4-6. Figure 4 shows the E and H plane radiation patterns for the feed when it is excited by a pure TE_{11} mode. The calculated gain is 22.4 dBi, and fairly good pattern circular symmetry is obtained. A reduction of the H plane sidelobes, and improved pattern symmetry should be obtainable by further refinement of the corrugation profile. For a TE_{11} mode incident on the feed each of the reflected modes is found to be at a level of at least -43 dBc. (Here dBc references the power level to that of the forward traveling TE_{11} mode.) These small values for the reflected modes are due to the fact that the waveguide diameter is very large with respect to the wavelength. The feed radiation pattern for the case when the TM_{11} mode is incident on the feed is shown in Fig. 5. For this case we find that the pattern is grossly asymmetric, with the maximum gain of 17.7 dBi, occurring in the E plane at $\Theta \cong 16°$. The on-axis gain of the feed is 13.7 dBi, or about 4 dB below the maximum. We may also note that when this pattern illuminates the subreflector $|\Theta| \leqslant 15°$, much of the power is lost in spillover. The pattern for each spurious mode may be calculated similarly, and some general comments can be made. Higher order TM modes have maximum gain points in the E plane, and TE modes in the H plane. As the mode number increases, the point of maximum gain moves out further from the feed axis, $\Theta = 0°$. For modes higher than TE_{13} less than 5% of the power in each mode is intercepted by the subreflector. This would indicate that the higher order spurious modes will have a smaller effect on the overall antenna gain than the lower order modes. Finally, an example of the feed pattern for the case when a mixture of modes excites the feed is shown in Fig. 6. The results are for a mode mixture where 6% of the incident power is carried by the TM_{11} mode, and 94% by the TE_{11} mode with the phase of TM_{11} mode with respect to the TE_{11} mode being 145°. The maximum gain occurs on the feed axis, and is 21.6 dBi, or about 0.8 dB below the gain for the case when a pure TE_{11} mode was incident. In a similar way, the feed pattern for an arbitrary combination of input modes may be calculated. It should be noted that modes without one azimuthal variation, that is, other than TE_{1n} and TM_{1n}, produce feed patterns which are hollow; i.e., no radiation on the feed axis is produced. The point of maximum gain moves further away from the axis as the mode number is increased.

B. Dual Reflector Patterns

The overall antenna patterns for the feed patterns of Figs. 4-6 were calculated using the method described in Sec. II Part C, and the results are plotted in Figs. 7-9. The calculated results are for the present 64-meter antenna system. The antenna far-field pattern in the E and H planes for a TE_{11} mode incident on the feed is shown in Fig. 7. The calculated gain is 86.15 dBi, and excellent pattern circular symmetry is obtained. The theoretical maximum gain of the system is 87.15 dBi. These calculations give an aperture efficiency, neglecting quadripod blockage and surface errors, of about -1 dB, or 79.5% for the TE_{11} mode. The calculated far field pattern for the TM_{11} case is shown in Fig. 8. The overall antenna pattern has a calculated on-axis gain of 62.1 dBi, with the maximum gain of 74.6 dBi occurring in the H plane at $\Theta \cong 0.009°$. The resulting pattern contains many sidelobes, and is very asymmetric. The result for the composition of modes 94% TE_{11} plus 6% TM_{11} with the correct phasing of TE_{11} at 0° and TM_{11} at 145° is shown in Fig. 9. The calculated axis gain for this composition is 85.78 dBi, or a loss of 0.4 dB from the TE_{11} case. This shows that if a given amount of microwave power were distributed between TE_{11} and TM_{11} in this ratio of power and in this phasing we would experience a loss of 0.4 dB (8.75%) in effective isotropically radiated power (EIRP) from the case where all the power was in the TE_{11} mode. The parameter of major interest for the Ka-band system is the EIRP, or equivalently the on-axis antenna gain for a given mode composition.

The on-axis antenna gain was calculated for each input mode to the feed. The results of these calculations are summarized in Table 1. We see that in terms of on-axis field effects, the modes TE_{12}, TM_{11}, and TM_{12} are of primary importance, the higher order modes being very poor on-axis radiators with respect to the TE_{11} mode. Modes of the type $m \neq 1$, i.e., TE_{0n}, TE_{2n}, TM_{2n} etc., may be considered by making a few simplificiations. If the Dual Reflector system were perfectly circularly symmetric it could be shown by symmetry considerations that modes with $m \neq 1$ do not contribute to the on-axis gain, i.e., the entry in Table 1 for these modes is $-\infty$. Depending upon their level and phase with respect to the TE_{11} mode they could cause the maximum gain to appear off-axis, although the on-axis field value would be the same as for that of the TE_{11} mode alone. Although the 64-meter system is not perfectly symmetric, it is assumed that the on-axis gain for these modes will be very small.

C. Efficiency Results

In this section we define an efficiency factor, η, which references the (EIRP) for a given mode content at the feed input to that for a pure TE_{11} mode incident on the feed. That is for a given RF power level, P_{RF}, and mode composition corresponding to an efficiency factor η, we have for the Effective Isotropically Radiated Power:

$$\text{EIRP}_{\text{dBw}} = P_{RF}\,(\text{dBw}) + 86.15\ \text{dB} + \eta(\text{dB}) \qquad (12)$$

The factor η depends upon the percentage of P_{RF} in each mode, and the phases of these modes. For a pure TE_{11} mode composition $\eta = 1.0 = 0$ dB. The results for η vs mode content are shown in Fig. 10. The horizontal axis represents the percent of TE_{11} mode present in the mode composition, or equivalently the total power level of the spurious modes with respect to the TE_{11} mode power. The vertical scale represents the efficiency factor η. Three curves are plotted, η_+, η_-, and η_f. For a given total spurious mode level η_- gives the minimum possible value for η and η_+ the maximum. The term η_f represents the effect of adding an ideal mode filter which dissipates all the spurious mode power and passes the TE_{11} power with no attenuation. In using Eq. (12) for this case, P_{RF} is the RF power measured before the filter.

For example, suppose the RF power is measured as 200 kW (53 dBw), and we also know that the RF power is 94% TE_{11} and 6% spurious modes (-12 dBc). Using Fig. 10 we find that for a spurious mode level of -12 dBc,

$$\eta_+ = -0.12\ \text{dB}$$
$$\eta_- = -0.4\ \text{dB} \qquad (13)$$

Then using Eq. (12), and realizing that the actual efficiency factor may fall anywhere between these two values, depending on which spurious modes are present and on their relative phases, we find

$$138.75\ \text{dBw} \leqslant \text{EIRP} \leqslant 139.03\ \text{dBw} \qquad (14)$$

If an ideal mode filter is added to dissipate all of the power carried by the spurious modes then

$$\eta_f = -0.18\ \text{dB} \qquad (15)$$

and

$$\text{EIRP} = 138.97\ \text{dBw} \qquad (16)$$

If we can only guarantee that the mode purity (TE_{11}%) is at least 94% then we must find the maximum value for η_+ and the minimum value for η_- for spurious mode levels less than -12 dBc (6%). Using Fig. 10 we find

$$\eta_+ = 0.02\ \text{dB}$$

and

$$\eta_- = -0.04\ \text{dB}$$

Using (12) we find

$$138.75\ \text{dBw} \leqslant \text{EIRP} \leqslant 139.17$$

The fact that $\eta_+ = 0.02$ dB (1.004) for some spurious mode level $\leqslant -12$ dBc deserves some comment. The result $\eta_+ > 1.0$ merely implies that there is a combination of modes that may be put into the feed that achieves slightly better illumination of the subreflector and paraboloid than the pure TE_{11} mode. An analogous effect is used in the dual mode horn where the power incident in the TE_{11} mode is redistributed between the TE_{11} and TM_{11} modes, and more efficient antenna illumination is obtained.

IV. Conclusions

The initial reason for performing this study was to determine some component specifications for the tube and transmission line making up the Ka-band system. Additional results regarding expected performance of the system were also provided by Varian Associates in the final report for the Ka-band feasibility study[2]. One of the comments made

[2]See D. Stone, R. Bier, M. Caplan, H. Huey, D. Pirkle, J. Robinson, and L. Thompson, *Feasibility Study for a 34 GHz (Ka-Band) Gyroamplifier, Final Report,* prepared by Varian Associates, Inc., under JPL subcontract #956813, Sept. 1984.

by Varian in the report is that even with the most careful tube design spurious mode levels of about -12 dBc are expected and that further mode purity can only be obtained by absorbing some of the RF power in a lossy mode filter. In addition, calculations on the effect of tilt alignment of the transmission line show that in order to maintain a total spurious mode level of less than -15 dBc, an optical bench arrangement will be necessary to align the components. For the case analyzed in detail in Section III, 94% TE_{11} and 6% spurious power, it was shown that a net gain in EIRP of only 0.22 dB was possible (assuming the worst case phasing of the spurious modes) by adding an ideal mode filter. More detailed calculations of helix mode filter performance indicate that with reasonable values for tolerances of the device parameters the insertion loss for the TE_{11} mode is about 0.1 dB, even with perfect conductivity assumed in the helical windings. Real life effects such as finite conductivity in these windings will also contribute to the TE_{11} insertion loss. Therefore, with real effects taken into account an optimistic estimate for the maximum increase in efficiency that could be expected by adding a filter is about 0.1 dB ($\sim$ 2%).

For the reasons mentioned above, it has been decided that a more reasonable specification for mode purity to be given to the tube designer is -12 dBc (94%), rather than the original -30 dBc (99.9%). This would eliminate the need for an optical bench system and also eliminate the development of a TE_{11} mode filter.

References

1. Bhanji, A., Hoppe, D., Hartop, R., Stone, E., Imbriale, W., Stone, D., and Caplan, M. High power Ka-band transmitter for planetary radar and spacecraft uplink, *TDA Progress Report 42-78* (April-June 1984), Jet Propulsion Laboratory, Pasadena, CA, pp. 24-48.

2. J. L. Hirshfield, Gyrotron, in *Infrared and Millimeter Waves*, Vol. 1, Academic Press, New York, pp. 1-54, 1979.

3. G. L. James, Analysis and design of TE_{11} to HE_{11}, corrugated cylindrical waveguide mode converters, *IEEE Trans. Microwave Theory and Tech.*, Vol. MTT-29, pp. 1059-1066, October 1981.

4. A. C. Ludwig, Radiation pattern synthesis for circular aperture horn antennas, *IEEE Trans. Antennas and Propagation*, Vol. AP-14, pp. 434-440, July 1966.

5. S. Silver, *Microwave Antenna Theory and Design*, Rad. Lab ser., Vol. 12, McGraw Hill, New York, pp. 336-338, 1949.

6. Veruttipong, T., Rochblatt, D., Imbriale, W., and Galindo, V., "Dual Shaped and Conic GTD/Jacobi-Bessel Analysis Programs," JPL-D-2096 (internal document), December 1984, Jet Propulsion Laboratory, Pasadena, CA.

7. Raj Mittra, Yahya Rahmat-Samii, Victor Galindo-Israel, and R. Norman, An efficient technique for the computation of vector secondary patterns of offset paraboloid reflectors, *IEEE Trans. Antennas and Propagation*, Vol. AP-27, pp. 294-304, May 1979.

8. R. E. Collin, *Foundations for Microwave Engineering*, McGraw Hill, New York, pp. 174-176, 1966.

Table 1. On-axis antenna gain for various modes incident on the feed

Input Mode	Gain, dBi	Gain Relative to the TE_{11} Mode, dB
TE_{11}	86.15	0
TM_{11}	62.1	−24.05
TE_{12}	60.2	−25.95
TM_{12}	61.5	−24.65
TE_{13}	~44	~−42
TM_{13}	~40	~−46
TE_{14}	~30	~−56
TM_{14}	~53	~−33
TE_{15}	~46	~−40

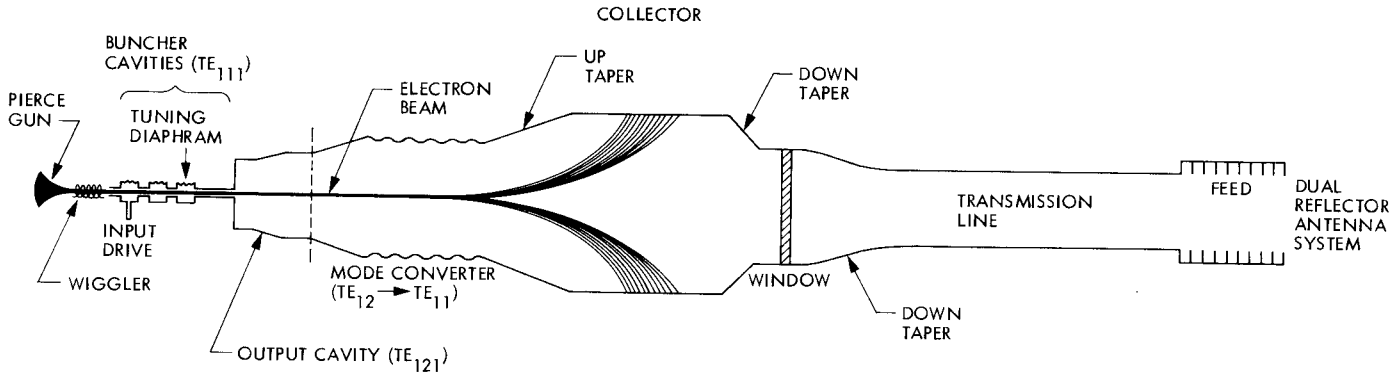

Fig. 1. Schematic of proposed gyroklystron and transmission line

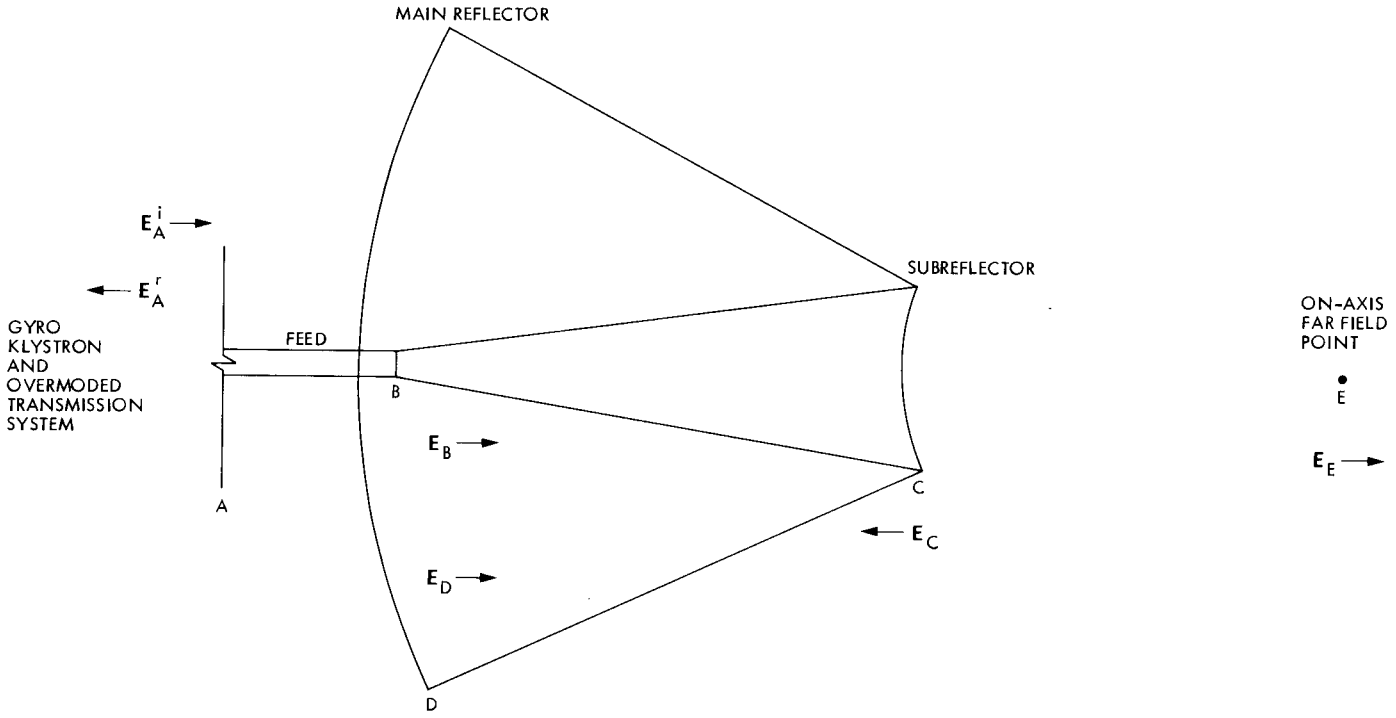

Fig. 2. Schematic of the feed and dual reflector system

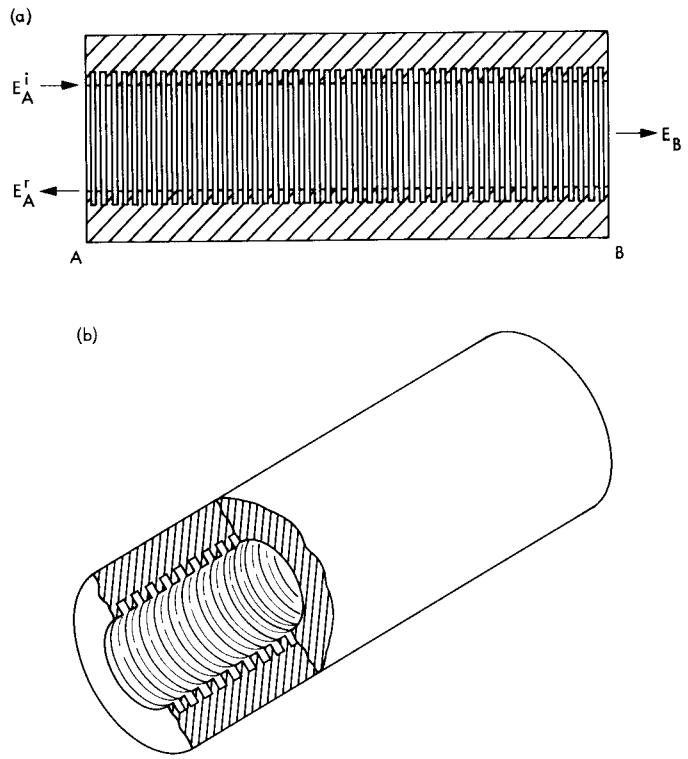

Fig. 3. Antenna feed, corrugated section with varying slot depth: (a) cross section view; (b) cut-away view

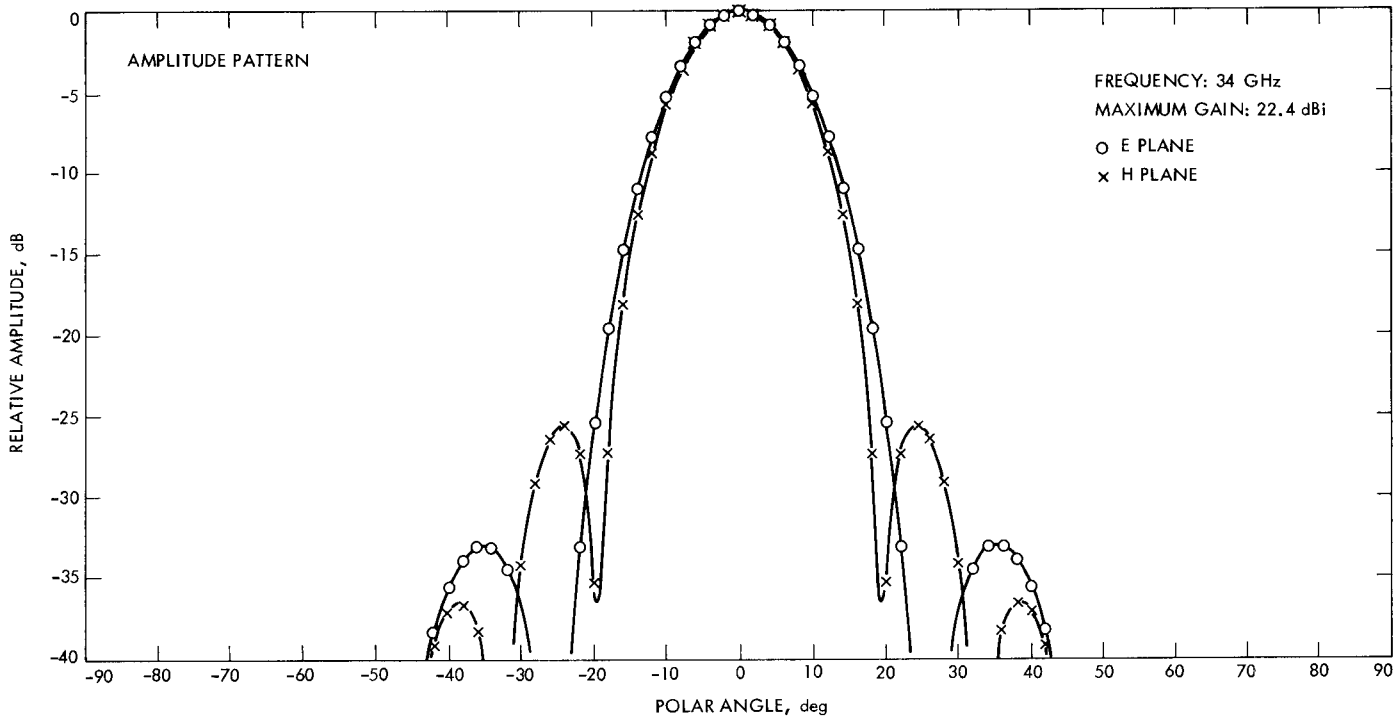

Fig. 4. Feed radiation patterns for a pure TE_{11} mode incident on the feed

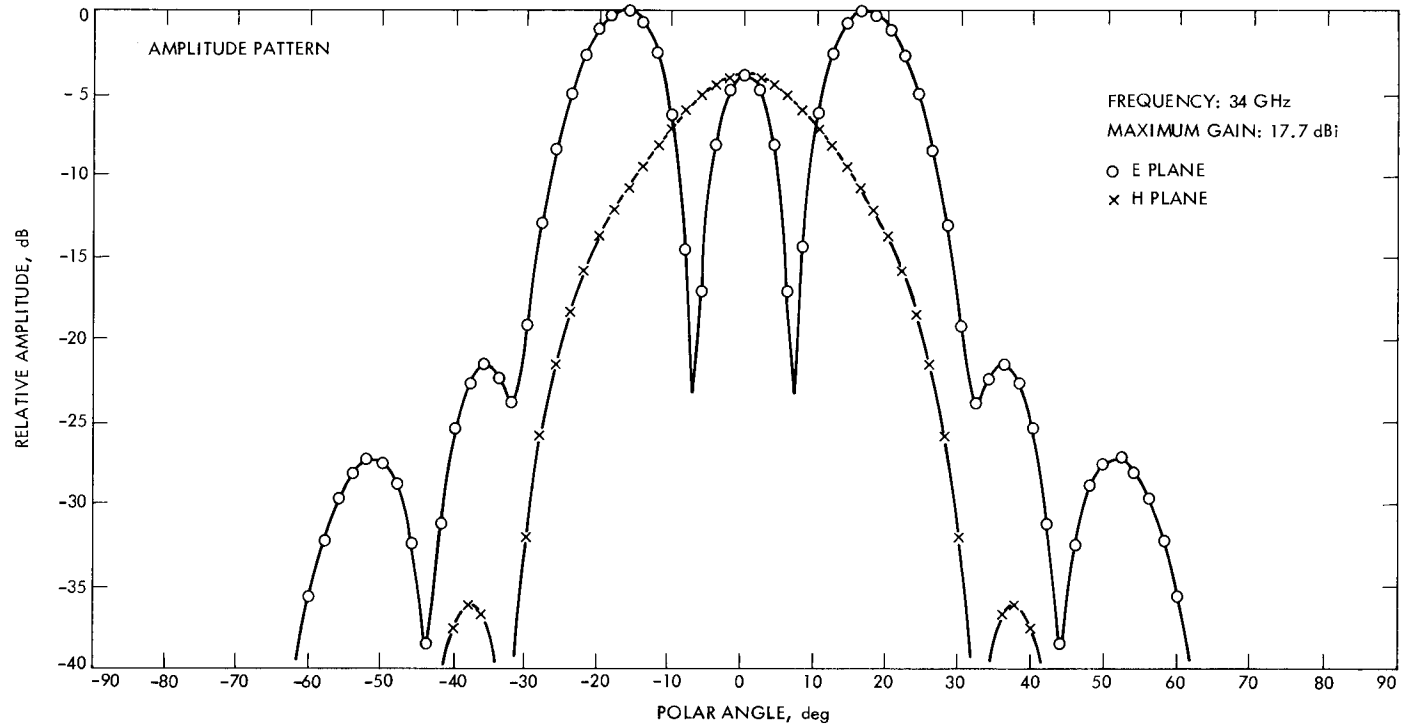

Fig. 5. Feed radiation patterns for a pure TM_{11} mode incident on the feed

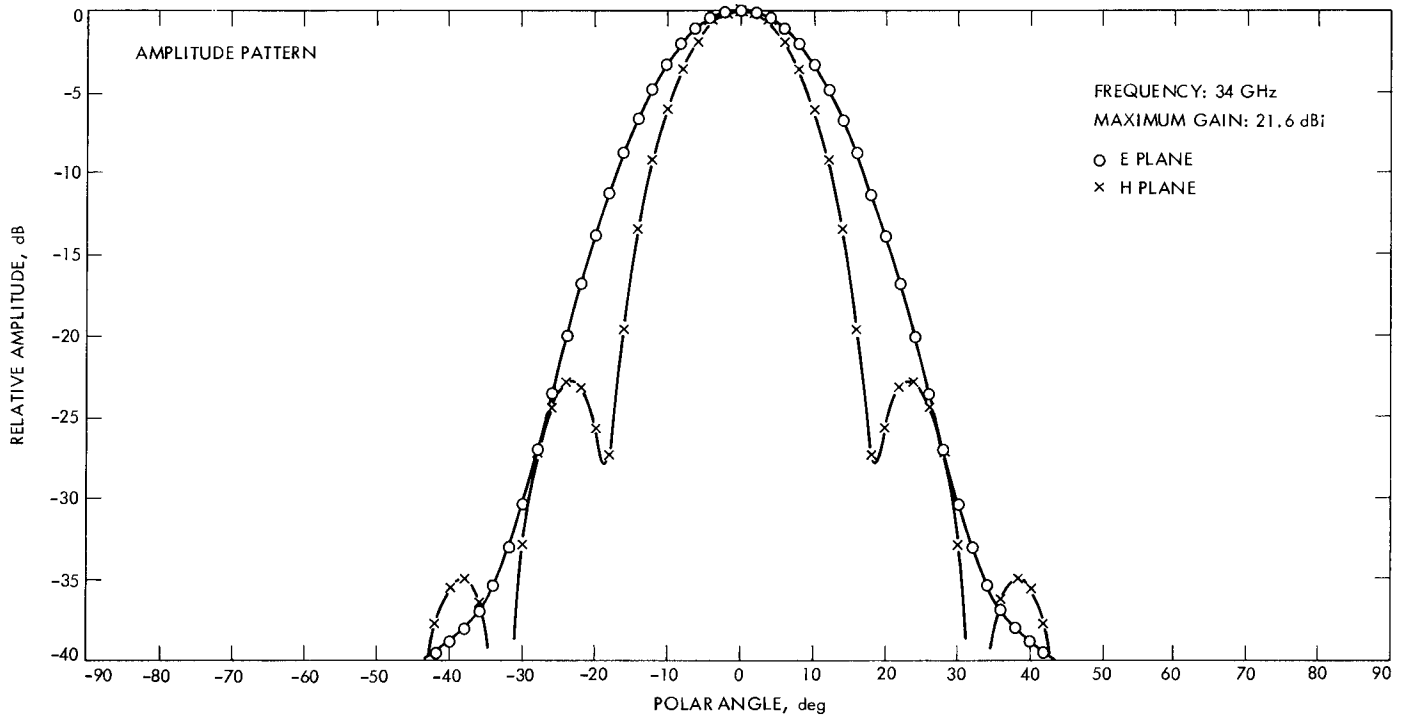

Fig. 6. Feed radiation patterns when a mixture of TE_{11} and TM_{11} modes is incident on the feed

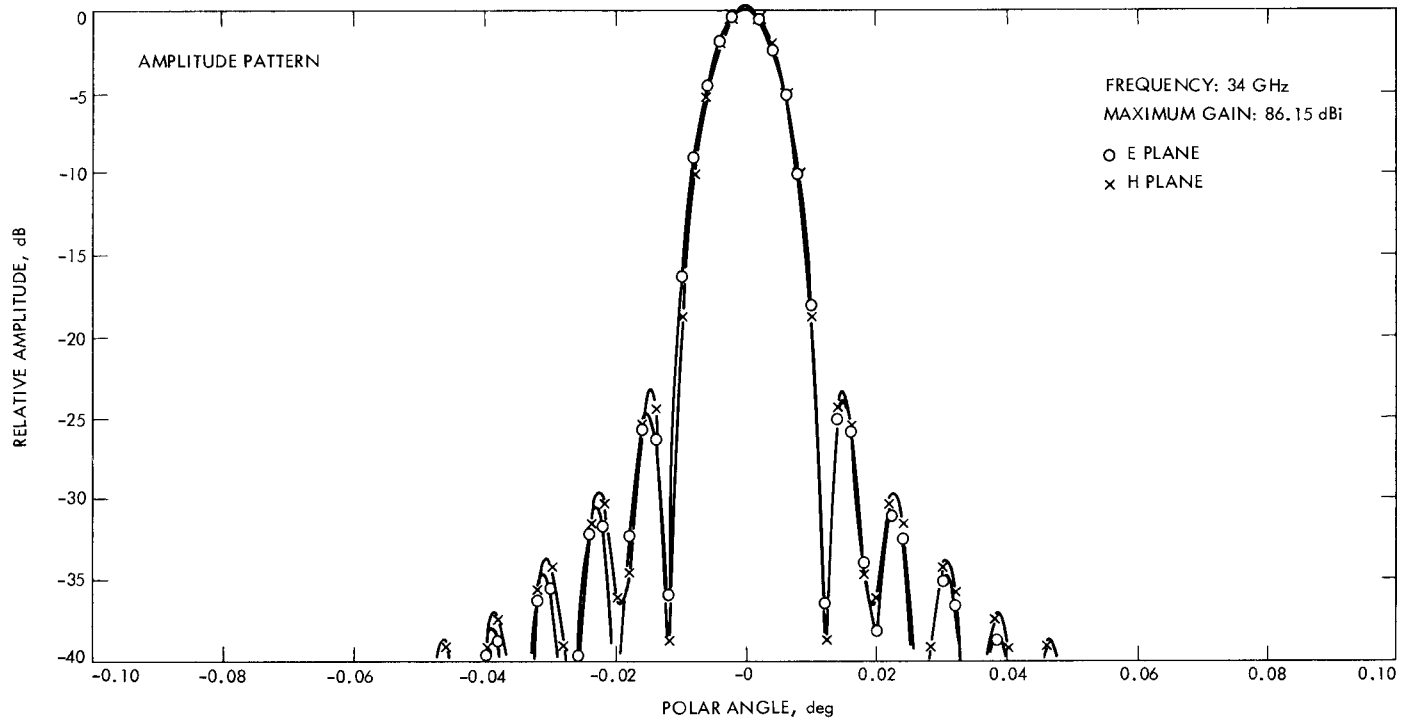

Fig. 7. Radiation patterns for the antenna when a pure TE_{11} mode is incident on the feed

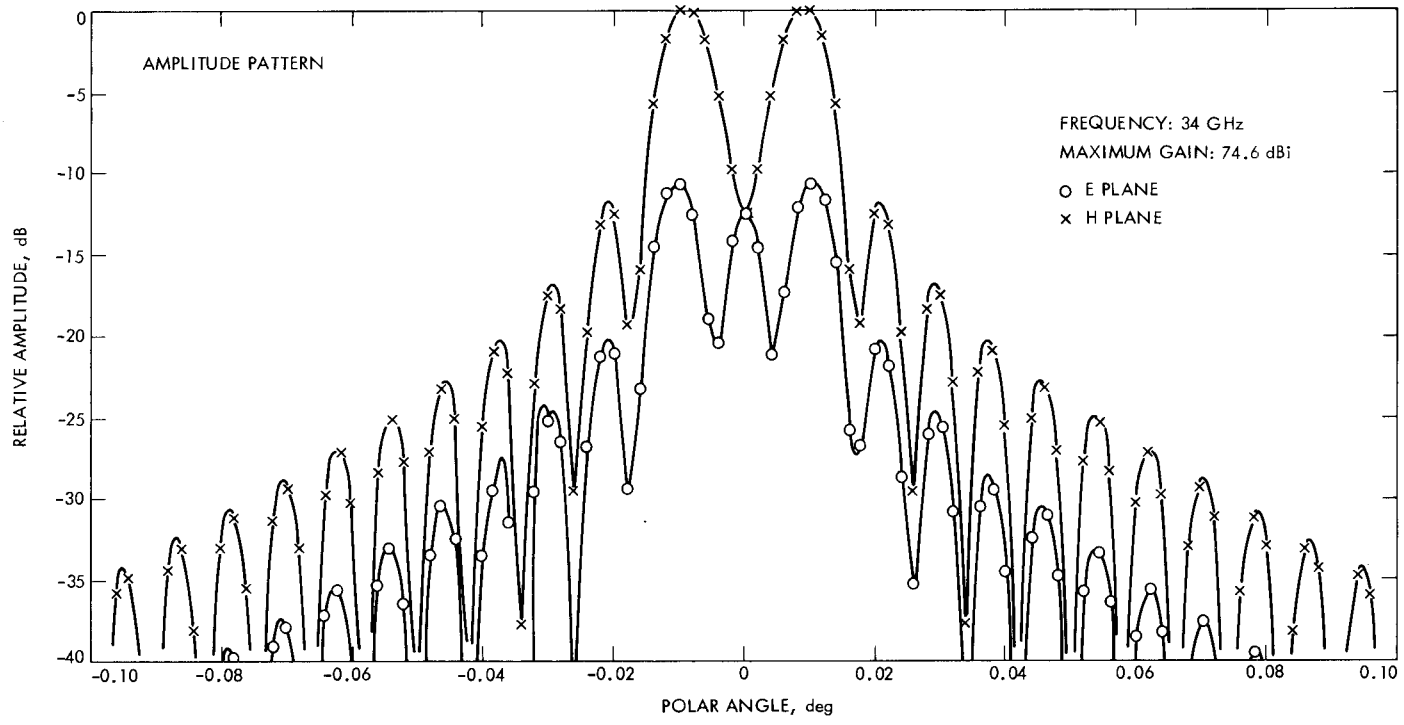

Fig. 8. Radiation patterns for the antenna when a pure TM_{11} mode is incident on the feed

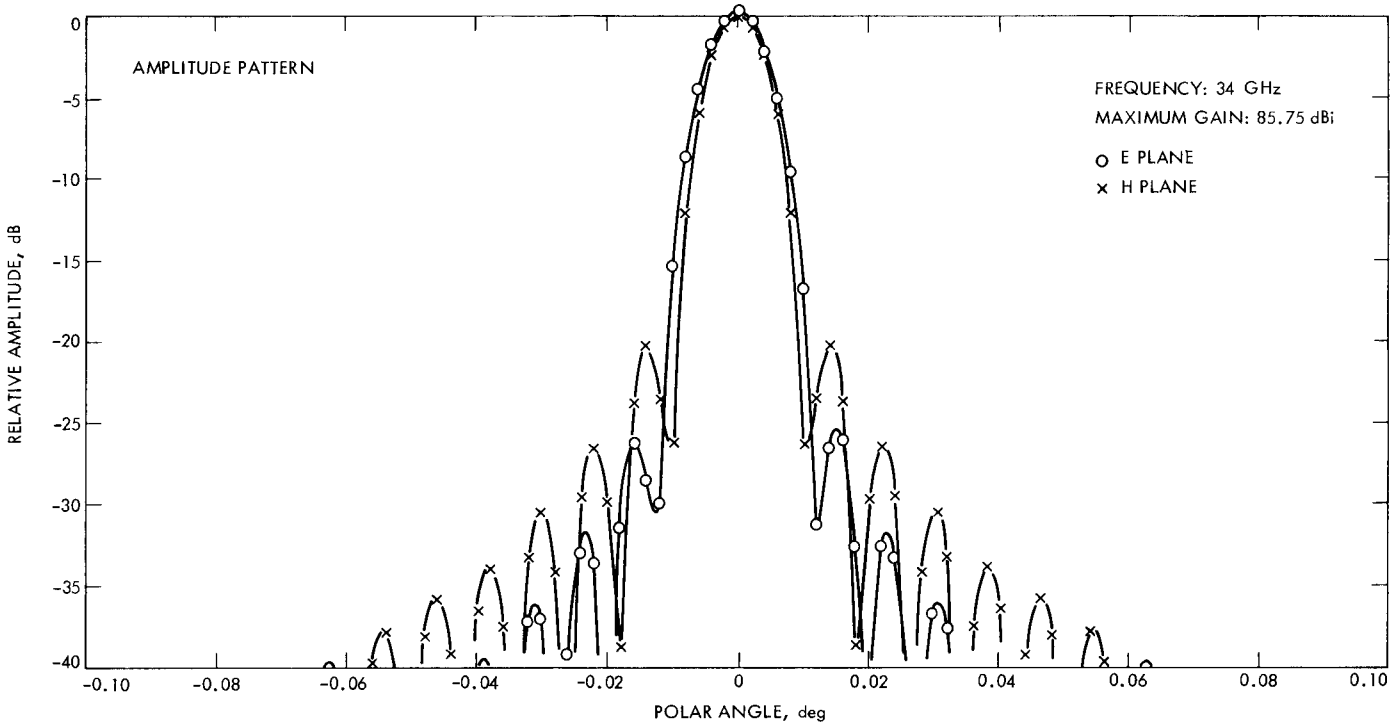

Fig. 9. Radiation patterns for the antenna when a mixture of TE_{11} and TM_{11} modes is incident on the feed

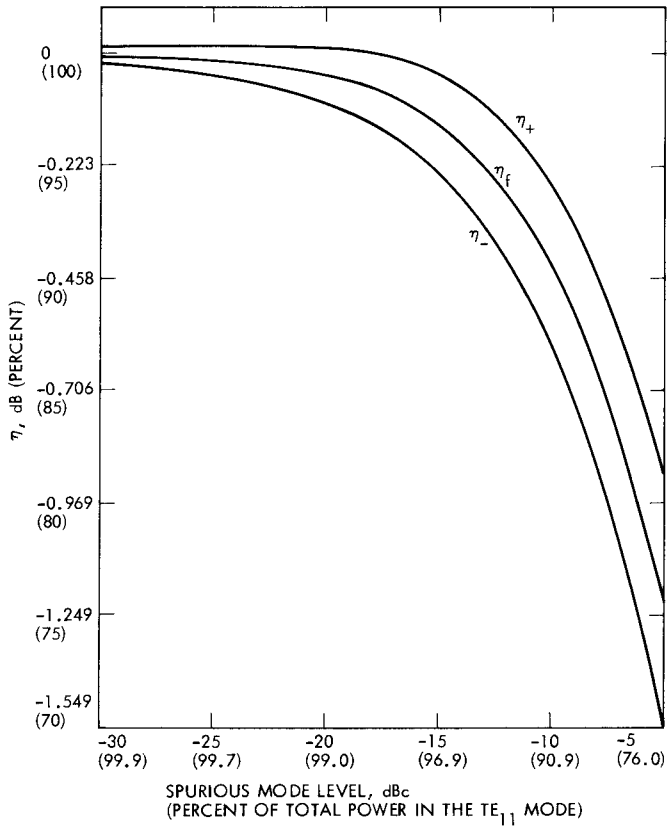

Fig. 10. Efficiency factors as a function of mode purity